

1 **Full Title**

2 Estimating dengue transmission intensity from serological data: a comparative analysis
3 using mixture and catalytic models.

4

5 **Short Title**

6 Comparing mixture and catalytic models.

7

8 **Authors**

9 Victoria Cox¹, Megan O'Driscoll^{1,2}, Natsuko Imai¹, Ari Prayitno³, Sri Rezeki Hadinegoro³,
10 Anne-Frieda Taurel⁴, Laurent Coudeville⁵, Ilaria Dorigatti¹.

11 **1** MRC Centre for Global Infectious Disease Analysis, School of Public Health, Imperial
12 College London, London, United Kingdom, **2** Department of Genetics, University of
13 Cambridge, Cambridge, United Kingdom, **3** Department of Child Health, Faculty of Medicine
14 Universitas Indonesia, Jakarta, Indonesia, **4** Sanofi Pasteur, Singapore, **5** Sanofi Pasteur,
15 Lyon, France.

16 **Abstract**

17 **Background.** Dengue virus (DENV) infection is a global health concern of increasing
18 magnitude. To target intervention strategies, accurate estimates of the force of infection
19 (FOI) are necessary. Catalytic models have been widely used to estimate DENV FOI and
20 rely on a binary classification of serostatus as seropositive or seronegative, according to pre-
21 defined antibody thresholds. Previous work has demonstrated the use of thresholds can
22 cause serostatus misclassification and biased estimates. In contrast, mixture models do not
23 rely on thresholds and use the full distribution of antibody titres. To date, there has been
24 limited application of mixture models to estimate DENV FOI.

25 **Methods.** We compare the application of mixture models and time-constant and
26 time-varying catalytic models to simulated data and to serological data collected in Vietnam
27 from 2004 to 2009 ($N \geq 2178$) and Indonesia in 2014 ($N = 3194$).

28 **Results.** The simulation study showed greater estimate bias from the time-constant
29 and time-varying catalytic models (FOI bias = 1.3% (0.05%, 4.6%) and 2.3% (0.06%, 7.8%),
30 seroprevalence bias = 3.1% (0.25%, 9.4%) and 2.9% (0.26%, 8.7%), respectively) than from
31 the mixture model (FOI bias = 0.41% (95% CI 0.02%, 2.7%), seroprevalence bias = 0.11%
32 (0.01%, 3.6%)). When applied to real data from Vietnam, the mixture model frequently
33 produced higher FOI and seroprevalence estimates than the catalytic models.

34 **Conclusions.** Our results suggest mixture models represent valid, potentially less
35 biased, alternatives to catalytic models, which could be particularly useful when estimating
36 FOI and seroprevalence in low transmission settings, where serostatus misclassification
37 tends to be higher.

38 **Author summary**

39 Characterising the transmission intensity of dengue virus in different geographic areas over
40 time is essential to understand who is at greatest risk of infection, and to inform the
41 implementation of interventions, such as vector control and vaccination. It is therefore
42 important to understand how methodological differences and model choice may influence
43 estimates of transmission intensity. We compared the application of catalytic and mixture
44 models to calculate the force of infection (FOI) of dengue virus from antibody titre data. We
45 observed greater bias in FOI estimates obtained from catalytic models than from mixture
46 models in areas where the transmission intensity was low. In high transmission intensity
47 areas, catalytic and mixture models produced consistent estimates. Our results indicate that
48 in low transmission settings, when antibody titre data are available, mixture models could be
49 preferential to estimate dengue virus FOI.

50 Introduction

51 Dengue fever is caused by infection with one or more of four antigenically distinct
52 serotypes of dengue virus (DENV1-4); a *Flavivirus* carried by *Aedes* mosquitoes (1,2).
53 DENV infects approximately 105 million people each year (3), primarily in tropical and sub-
54 tropical regions. The geographical range of DENV is increasing (1,4,5) and it is expected
55 that the spread of dengue will be influenced by rising global temperatures and increasing
56 urbanisation (1,6). Intervention measures to date rely essentially on vector control due to the
57 absence of antiviral treatment, challenges in the use of the first licensed dengue vaccine for
58 widespread dengue prevention and control (7), as well as in the use of rapid diagnostic tests
59 for screening (8). The current and expected future burden of dengue on health-systems is
60 therefore high, demonstrating a continuing need for increased understanding of DENV
61 transmission.

62 Estimating epidemiological parameters such as the force of infection (FOI, the per
63 capita rate at which a susceptible person is infected) and population seroprevalence (the
64 proportion of people in a population exposed to a virus, as determined by the detection of
65 antibodies in the blood) allow us to gain insights into the subsets of populations most at risk
66 of infection and disease (9), to assess the predicted impact of an intervention strategy (10),
67 and to inform public health policy (11,12).

68 Both the FOI and seroprevalence can be estimated using mathematical models
69 calibrated to serological data measuring IgG antibody levels (also called titres) from blood
70 samples. IgG titres are obtained using Enzyme-Linked Immunosorbent Assays (ELISAs) and
71 are often classified into qualitative, binary test results (seropositive or seronegative) based
72 on the manufacturer's threshold.

73 Catalytic models, first proposed in 1934, estimate disease FOI from age-stratified
74 serological or case notification data (13). In these models, large rates of increase in
75 seroprevalence between individuals who are age a versus age $a+1$ are explained by high

76 age-specific FOI (assuming the FOI is constant in time) or high time-specific FOI
77 experienced by individuals of all ages during the period a to $a+1$ years ago (14). Catalytic
78 models have been used extensively for measles (15), rubella (16), Hepatitis A (17), Chagas
79 disease (18), and DENV (12,14,19–21). Whilst commonly used, Bollaerts *et al.* and Vink *et*
80 *al.* (22,23) suggest that catalytic models risk generating biased estimates due to data-loss
81 and/or mis-classification. For example, samples with titres greater than the seronegative
82 threshold but lower than the seropositive threshold are classified as ‘equivocal’ and
83 discarded from the analysis. Furthermore, titre levels of seropositive individuals in a given
84 population may be affected by factors including host response, the degree of exposure to the
85 pathogen and infection timing, which could lead to misclassification.

86 Mixture models are flexible statistical models that can be applied to continuous data
87 from different clusters or populations, called components. Mixture models can therefore be
88 applied to the absolute antibody titre values in serology datasets, rather than to the counts of
89 titres in each of two classes (seropositive/seronegative) as is necessary for catalytic models
90 (22). The components’ distributions and their defining parameters (e.g., the mean titre of
91 each component distribution) are inferred from a fitted mixture model which is used to
92 estimate the FOI and population seroprevalence (22,24). To date, mixture models have been
93 applied to serological data to estimate the seroprevalence of infectious diseases such as
94 parvovirus B19 and rubella in England (25,26), human papillomavirus in the Netherlands
95 (23), measles in Italy (27), and a selection of arboviruses including DENV in Zambia (28). In
96 addition, mixture models have been used to develop a framework capable of distinguishing
97 between primary and post-primary DENV infections (29) and to estimate the FOI of
98 Varicella-Zoster virus in Belgium (22). However, these methods have not been used to
99 estimate DENV FOI. Here, we present the results of a simulation study and a comparison of
100 the DENV transmission intensity estimates obtained from mixture and catalytic models
101 applied to age-stratified serological datasets from Vietnam ($N \geq 2178$, for years 2004-2009)
102 and Indonesia ($N = 3194$, for 2014).

103 **Methods**

104 **Data**

105 **Age-stratified seroprevalence data.** DENV IgG data were collected in Long Xuyen,
106 Vietnam, during a prospective epidemiological study that was conducted to assess the
107 suitability of the area for future CYD-TDV vaccine efficacy trials, as described previously
108 (30). Samples were collected from children under 11 years old in 2004 and then from
109 children under 15 years old during September to February in 2004-2005, 2005-2006, 2006-
110 2007, 2007-2008 and 2008-2009 (Datasets A-1 to A-6, Table 1). The titres were measured
111 using in-house ELISA assays (Arbovirus Laboratory of Pasteur Institute, Ho Chi Minh City).

112 **Table 1: Description of the datasets used in the analyses.** Summary statistics including
113 notation, region, the assay used, the year of testing, the age range of the children
114 participating to the study and the sample sizes.

Dataset	Region	Assay type	Year	Age Range	Sample Size
A-1	Long Xuyen, Vietnam	IgG ELISA	2004	3-10	2,178
A-2	Long Xuyen, Vietnam	IgG ELISA	2004-2005	3-13	3,681
A-3	Long Xuyen, Vietnam	IgG ELISA	2005-2006	3-14	3,727
A-4	Long Xuyen, Vietnam	IgG ELISA	2006-2007	3-14	3,651
A-5	Long Xuyen, Vietnam	IgG ELISA	2007-2008	4-14	2,959
A-6	Long Xuyen, Vietnam	IgG ELISA	2008-2009	5-14	2,249
B	30 urban subdistricts, Indonesia	IgG ELISA	2014	1-18	3,194
C	Simulated data	Simulated	N/A	1-18	3,194

115

116 DENV IgG data from 30 urban subdistricts in Indonesia were collected from children
117 under 18 years old as part of a cross-sectional seroprevalence survey in 2014 (31) (Dataset

118 B). The total number of participants was 3,194 (see Supplementary Data for subdistrict
119 information). IgG titres were measured using the commercial Panbio® Dengue IgG Indirect
120 ELISA kit.

121 **Simulated datasets.** We simulated 200 antibody titre datasets (Dataset C), with the
122 same age-distribution and sample size as the Indonesian seroprevalence survey data
123 (Dataset B). For each simulation the distributions used for sampling seronegative and
124 seropositive antibody titres were randomly selected from a normal, gamma or Weibull
125 distribution. This gave 9 possible combinations of distribution pairs for seronegative and
126 seropositive antibody titre values per simulation. Normal, gamma and Weibull distributions
127 were chosen based on preliminary work where mixture models applied to our antibody titre
128 datasets most commonly fitted one of these three distributions. Parameter values were
129 randomly drawn from uniform distributions with limits as shown in S2 Table. The serostatus
130 of each individual was drawn from a Bernoulli distribution with probability $1 - e^{-\lambda a}$, where a
131 is the age of the individual and λ is the FOI. FOI was assumed to be constant with age and
132 time. Titre values for each individual were subsequently randomly drawn from the respective
133 component distributions. The analysis was conducted in the statistical programming
134 language R (32).

135 **Ethics statement.** Ethical approval for the secondary analysis of the age-stratified
136 seroprevalence datasets was granted by the Imperial College Research Ethics Committee
137 (Approval Reference 21IC7066).

138

139 **Catalytic model**

140 **Data preparation.** Catalytic models rely on data that are binarily classified as
141 seropositive or seronegative. For Datasets A-1 to A-6, a background/control titre (t) was
142 measured for each assay. An individual titre was classified as seronegative if $t \leq t$ and
143 seropositive otherwise. For Dataset B, samples with titres ≤ 9 PanBio units were classified

144 as seronegative and ≥ 11 as seropositive. Titres >9 and <11 were discarded (28 out of 3,194
145 samples). For simulated Dataset C, titres were classified as seronegative if they were $\leq X$
146 and seropositive if they were $\geq Y$. X and Y are thresholds that were optimised using the ‘true’
147 simulated serostatuses: the *optim* function in R, using the Nelder Mead algorithm, was used
148 to calculate the X and Y values per simulated dataset resulting in the fewest titre
149 misclassifications. The mean number of samples discarded (titre value $>X$ and $<Y$) per
150 simulation was 1.06 out of 3194 (median = 0, interquartile range (IQR) = 1, range = 0 to 19).
151 The mean percentage of titres misclassified across the simulations was 2.4% (median =
152 0.6%, IQR = 2.0%, range = 0% to 69.4%).

153 **Parameter estimation.** We used the same catalytic model developed in Rodriguez-
154 Barraquer *et al.*, 2011 (33). The proportion of seropositive individuals in age group i ($\pi(a_i)$),
155 was estimated as in Equation 1, where $\lambda(a_i)$ denotes the FOI, i.e. the per-capita rate of
156 infection experienced by individuals in age group i , and a denotes the age (14).

$$157 \quad \pi(a_i) = 1 - \exp(-\lambda(a_i) * a) \quad \text{[Equation 1]}$$

158 A binomial log-likelihood was assumed for the FOI (Equation 2), where N_i is the total number
159 of individuals and X_i is the number of seropositive individuals in age group i (19). The
160 maximum likelihood estimate of the FOI parameter is estimated as shown in Equation 2
161 using the *optim* function in R.

$$162 \quad \ln L(\lambda(a_i)) = \sum_i [(N_i - X_i)(\log(1 - \pi(a_i))) + X_i(\log(\pi(a_i)))] \quad \text{[Equation 2]}$$

163 When we assume the FOI is time-varying, the estimated $\lambda(a_i)$ values were averaged
164 across the age groups (number of age groups = n) to give the mean yearly FOI experienced
165 over the study period (Equation 3). When we assume the FOI is constant with time, $\lambda(a_i)$
166 equals λ .

$$167 \quad \lambda = \frac{\sum_i \lambda(a_i)}{n} \quad \text{[Equation 3]}$$

168 We estimated 95% Confidence Intervals (CI) using a bootstrap method, where the data were
169 sampled with replacement 1000 times. The 95% CI was given by the 2.5% to 97.5%
170 quantiles of the estimates from the bootstrap samples.

171 **Mixture model**

172 **Applying the mixture models to the titre distributions.** Mixture models were
173 applied to the bimodal distribution of individual antibody titres as described in Bollaerts *et al.*,
174 2012 and Hens *et al.*, 2012. The model defines the distribution of the log(titres + 1) (Z) as a
175 mixture of two distinct distributions: one for susceptible individuals (seronegative, Z_S) and
176 one for individuals who have been previously infected (seropositive, Z_I). The two-component
177 mixture model is represented by:

$$178 f(z | z_S, z_I, a_i) = (1 - \pi(a_i))f_S(z_S | \mu_S, \sigma_S) + \pi(a_i)f_I(z_I | \mu_I, \sigma_I) \quad \text{[Equation 4]}$$

179 where f_S and f_I represent the probability density function of the seronegative and
180 seropositive components, respectively, and where μ and σ represent the mean and standard
181 deviation of each component. The age-dependent mean log(titre+1) ($\mu(a_i)$) is calculated as in
182 Equation 5, which corresponds to an expression for the age-specific seroprevalence ($\pi(a_i)$)
183 (Equation 6).

$$184 \mu(a_i) = (1 - \pi(a_i))\mu_S + \pi(a_i)\mu_I \quad \text{[Equation 5]}$$

$$185 \pi(a_i) = \frac{\mu(a_i) - \mu_S}{\mu_I - \mu_S} \quad \text{[Equation 6]}$$

186 The age-dependent FOI, $\lambda(a_i)$, can be derived from the seroprevalence as described
187 in Equation 7 (22) and in turn can be expressed as a function of the underlying antibody titre
188 distribution as shown in Equation 8, where $\mu'(a_i)$ represents the derivative of the age-specific
189 mean log(titre+1). The age-dependent FOI can be averaged across the age groups to give
190 the total FOI, λ (Equation 3).

191
$$\lambda(a_i) = \frac{\pi'(a_i)}{1 - \pi(a_i)} \quad \text{[Equation 7]}$$

192
$$\lambda(a_i) = \frac{\mu'(a_i)}{\mu_I - \mu(a_i)} \quad \text{[Equation 8]}$$

193 The *mixdist* R package (34) was used to fit the mixture models to the titre data using
194 an Expectation Maximisation (EM) algorithm. The package was adapted to allow fitting of
195 different distributions for the seronegative and seropositive titre components: normal,
196 gamma and Weibull distributions were fitted for each component, giving 9 possible
197 combinations. The model giving the best fit to the titre distribution (determined by minimising
198 the log-likelihood ratio statistic) among the 9 combinations tested was chosen and its
199 estimates of the means (μ_s and μ_I) and standard deviations (σ_s and σ_I) for the seronegative
200 and seropositive components were extracted (and for Dataset C they were compared, as
201 well as the FOI, λ , against the true simulated parameter values). We explored multiple
202 parameterisations, including fixing the standard deviation of the two mixture components.
203 For the Vietnamese datasets, we optimised the model having constrained the standard
204 deviation of the seropositive component to multiple different values (for Dataset A-4 we set
205 σ_I equal to all values from 0.02 to 0.08 in steps of 0.01, for the other five Datasets we set σ_I
206 equal to all values from 0.05, to 0.15 in steps of 0.01). For the Indonesian dataset (Dataset
207 B) the standard deviations of both components were constrained (σ_s was set equal to 0.10
208 to 0.15 in steps of 0.001, and σ_I was set equal to 0.15 to 0.3 in steps of 0.05).

209 **Parameter estimation.** The distribution mean, $\mu(a)$, was estimated by least-squares
210 regression using a monotonically increasing P spline fitted to the age-stratified log(titre+1)
211 data (22,24,35). Equally spaced cubic polynomial segments (degree = 3) made up the
212 spline. The optimal smoothing parameter (α) and number of segments (knots) were
213 determined using the Bayesian Information Criterion, having explored combinations of α
214 values (set equal to 0.001, 0.01, 0.1, 0.5, 1, 5, 10, 50, 100, 500) and knots (set equal to
215 values in the sequence: 5 to the maximum number of x-axis age categories, step size = 1).

216 The spline was fitted using the *mpspline.fit* function from the *serostat* R package (36). The
217 $\mu'(a)$ term for the FOI estimation was calculated by taking the gradient of the fitted spline at
218 each age. The 95% CI around the parameter estimates were calculated using a bootstrap
219 method, as described above. Code to recreate the simulated datasets and to run the mixture
220 model analysis are available at: <https://github.com/Tori-Cox/Mixture-catalytic-models>.

221

222

223 Results

224 **Simulated data.** The mixture model identified the correct distributions used to simulate
225 both seropositive and seronegative titres in 50% (100/200) of simulations, one of the two
226 distributions in 42.5% (85/200) of simulations and did not correctly identify either distribution
227 in 7.5% (15/200) of the simulations. In all 15 simulations where neither distribution was
228 correctly identified, the seronegative titre values were drawn from the Weibull distribution (S3
229 Table). The estimated 95% CIs contained the true parameter values used to simulate the
230 data in 87% (174/200), 92% (184/200), 80.5% (161/200) and 90.5% (181/200) of simulations
231 for μ_S , μ_I , σ_S and σ_I , respectively (S5 Figure).

232 The mixture model correctly estimated the FOI for 99% (198/200) and the
233 seroprevalence for 97.5% (195/200) of simulations. The time-varying catalytic model
234 correctly estimated the FOI for 98% (196/200) and the seroprevalence for 85% (170/200) of
235 simulations. The time-constant catalytic model correctly estimated the FOI and
236 seroprevalence for 8.5% (17/200) and 16.5% (33/200) of simulations, respectively. The
237 estimates were categorised as correct if the estimated 95% CIs contained the true values. It
238 should be noted that the time-varying catalytic model produced wider CIs compared to when
239 assuming a constant-in-time FOI (Figure 1). Bias was calculated as the estimated parameter
240 values minus the true parameter values. Absolute bias in the FOI estimates (0.41% (95% CI
241 0.02%, 2.7%), 1.3% (0.05%, 4.6%) and 2.3% (0.06%, 7.8%) for the mixture, time-constant
242 and time-varying catalytic models, respectively) and the seroprevalence estimates (0.11%
243 (0.01%, 3.6%), 3.1% (0.25%, 9.4%) and 2.9% (0.26%, 8.7%)) was smaller for the mixture
244 model estimates (Figure 1).

245 The catalytic model under both assumptions underestimated the FOI and
246 seroprevalence, particularly at higher values (Figure 1 and Figure 2). High titre
247 misclassification error rates were positively associated with increased parameter estimate
248 bias in the catalytic models (S7 Figure). As expected, parameter estimate bias was reduced
249 when we fit the catalytic models to the simulated 'true serostatus' instead of classifying the

250 titres using optimised thresholds: the FOI was then correctly estimated for 99.5% (199/200)
251 and 48% (96/200) of simulations by the time-varying and time-constant FOI catalytic models,
252 respectively.

253 **Long Xuyen, Vietnam data.** When we applied the mixture model (Figure 3) to the data
254 from Long Xuyen, Vietnam, the total population-level seroprevalence estimates ranged from
255 16.3% (95% CI 13.8%-18.8%) in 2004 to 37.6% (24.9%-40.3%) in 2005-2006. The
256 seroprevalence estimates from the time-constant and time-varying catalytic models were
257 consistent with each other, with the latter ranging from 18.9% (16.3%-21.7%) in 2006-2007
258 to 29.9% (26.2%-33.7%) in 2008-2009. The seroprevalence estimates from all three models
259 were consistent (as determined by the 95% CIs) for 4 out of 6 datasets (Figure 4, S4 Table).
260 The general trend in the age-specific seroprevalence estimates, specifically for Datasets A-
261 2:A-5, differed significantly between the mixture model and the catalytic models, with the
262 mixture model estimating higher seroprevalence at the older ages (Figure 5).

263 The FOI estimates ranged from 2.6% (95% CI 1.9-3.3%) in 2004 to 9.9% (7.7%-12.4%)
264 in 2004-2005 for the mixture model and 2.4% (0.7%-5.8%) in 2006-2007 to 5.0% (1.2%-
265 11.8%) in 2004-2005 for the time-varying catalytic model. The FOI estimates from the
266 mixture model versus the time-varying catalytic model were consistent for 6 out of 6
267 datasets, and versus the time-constant catalytic model they were consistent for 3 out of 6
268 datasets (Figure 4, S4 Table). There is a higher degree of uncertainty around the estimates
269 from the catalytic model when assuming a time-varying FOI compared to the time-constant
270 FOI assumption (Figure 4). We observe greater differences in the estimates from each
271 model when comparing the age-specific FOI as opposed to the averaged total FOI (S9
272 Figure).

273 **Indonesian data.** The mixture and catalytic models fitted to the Indonesian data
274 produced consistent FOI, total population seroprevalence and age-specific seroprevalence
275 estimates. The FOI was estimated at 15.4% (95% CI: 10.6%-21.3%), 14.3% (13.6%-15.0%)
276 and 16.4% (2.2%-81.4%), and the seroprevalence at 71.8% (69.4%-74.1%), 70% (68.6%-

277 71.4%) and 70.0% (65.5%-74.3%) by the mixture model and the time-constant and time-
278 varying catalytic models, respectively (Figure 4, S4 Table).

279

280 Discussion

281 In our simulation study, the mixture model produced less biased estimates of FOI and
282 seroprevalence than the catalytic models (Figure 1). The catalytic models consistently
283 underestimated the parameters, particularly at higher values (Figure 2). Increased bias in the
284 catalytic model estimates was associated with increased serostatus misclassification (S7
285 Figure). Serostatus misclassification occurred more often in simulations where the mean
286 $\log(\text{titre} + 1)$ for the susceptible/seronegative component was higher and/or the mean
287 $\log(\text{titre} + 1)$ for the infected/seropositive component was lower (S6 Figure), indicating
288 greater overlap between the distributions of the two components. It is worth noting that the
289 apparent poor performance of the catalytic model is directly related to our choice of
290 simulated parameter values, and we would expect better performance when using
291 parameters that would have given clearer bimodal titre distributions, where serostatus
292 misclassification would have been lower.

293 Differences in the degree of overlap between components in real serological datasets
294 (S8 Figure) reflect differences in transmission intensity and variable degrees of
295 spatiotemporal heterogeneities in the risk of infection (3,37). In datasets collected from areas
296 which experience hyperendemic DENV circulation, one expects greater separation between
297 the titre components because most seropositive individuals likely have had multiple
298 infections, translating to higher antibody titres. In these instances, catalytic and mixture
299 models are expected to produce more similar estimates of FOI and seroprevalence as fewer
300 samples are misclassified during the qualitative, binary classification of the data needed to
301 calibrate catalytic models (22,38). This is consistent with the reduced variability we observe
302 in our FOI and seroprevalence estimates from each model when they were applied to
303 serological data from Indonesia compared to Vietnam, where the former had higher
304 separation of titre distributions (Figure 3, Figure 4, S4 Table).

305 The FOI for Indonesia was estimated at 15.4% (95% CI: 10.6%-21.3%), 14.3% (13.6%-
306 15.0%) and 16.4% (2.2%-81.4%), and the seroprevalence at 71.8% (69.4%-74.1%), 70%

307 (68.6%-71.4%) and 70.0% (65.5%-74.3%) by the mixture model and catalytic model under
308 the time-constant and time-varying FOI assumptions, respectively. The FOI estimates are
309 consistent with previously published results from catalytic models fitted to case-notification
310 data from 2008-2017 in Jakarta, Indonesia (13.0%, 95% CI: 12.9-13.1%) (12). The
311 seroprevalence estimates are consistent with previously published results using time-
312 constant catalytic models applied to the same serology dataset (Dataset B) (31,39). Our
313 results show that the mixture and catalytic models do not significantly differ in their FOI and
314 seroprevalence estimates in this setting.

315 The mixture model applied to the six datasets from Vietnam produced more variable
316 estimates (FOI range = 2.6%-9.9%, seroprevalence range = 16%.3-37.6%) than the catalytic
317 models (FOI range = 2.3%-3.7% and 2.4%-5.0%, seroprevalence range = 19.0%-30.0% and
318 18.9%-29.9% under the assumption of a time-constant or time-varying FOI respectively).
319 The estimates from the mixture model tended to exceed those obtained from the catalytic
320 models (Figure 4, S4 Table). Given the negative bias observed for the catalytic models in
321 our simulation study, we expect the higher mixture model estimates to be more accurate for
322 the Vietnamese setting. The higher FOI estimates are closer to previously published
323 estimates of 11.7% (95% CI: 10.8-12.7%) (40) using data collected from Binh Thuan
324 province in 2003, and 14.2% (95% CI: 12.9-18.4%) using data collected from Dong Thap
325 province in 1996-7 (19). Previous work has demonstrated large spatiotemporal
326 heterogeneity of DENV in Vietnam (37).

327 The variance between our mixture and catalytic model estimates for Vietnam is
328 greatest in the age-specific seroprevalence and FOI estimates (Figure 5, S9 Figure). As
329 expected, the time-varying catalytic model and the mixture model (which implicitly models
330 FOI as time-varying), are better able to capture the age-specific seroprevalence than the
331 time-constant catalytic model. However, the time-varying catalytic model produced less
332 stable estimates (wider CIs) than the time-constant catalytic model or the mixture model
333 (Figure 1 and Figure 2).

334 A major advantage of the mixture model is the comparative ease with which it can be
335 applied to serology data to estimate transmission intensity without the need to use
336 thresholds to process the data. Furthermore, to generate robust estimates, there are fewer
337 data requirements for mixture models than for catalytic models: in the former, the data are
338 pooled and age is used only to calculate the age-specific mean $\log(\text{titre} + 1)$ using a spline,
339 meaning that there are no constraints on the number of participants per age category.
340 However, it is important to consider the bias that will be introduced if the mixture distributions
341 fit the titre data poorly (38). Biggs *et al.* fit mixture distributions to DENV antibody titre data in
342 the Philippines to develop a framework distinguishing between post and primary DENV
343 infection (29) by specifying a three-component mixture for seronegative, seropositive with a
344 primary infection and seropositive with post-primary infections. In future work, it would be of
345 interest to explore the FOI estimates obtained on the Vietnamese datasets with a similar
346 three-component mixture model.

347 Our results suggest that mixture models represent a good alternative to catalytic
348 models to quantify DENV time-varying FOI and seroprevalence from age-stratified
349 serological data, with potentially less bias and less uncertainty. They may be particularly
350 useful when estimating FOI in low transmission settings and/or when the study population is
351 younger, where there is higher overlap between the component distributions (S8 Figure) so
352 the risk of serostatus misclassification and bias introduction when using cut-off threshold
353 methods is greater (S6 Figure and S7 Figure). We have provided code for both models to
354 encourage further exploration and comparison of the two methods. Critically, further
355 investigation of the use of mixture models depends on the availability of raw antibody titre
356 data. For these reasons, we would encourage current and future seroprevalence studies on
357 DENV as well as other infectious diseases, to publish anonymised individual-level antibody
358 titre data where it is possible to do so.

359

360 **Funding**

361 This work was supported by the MRC Centre for Global Infectious Disease Analysis
362 (reference MR/R015600/1), jointly funded by the UK Medical Research Council (MRC) and
363 the UK Foreign, Commonwealth & Development Office (FCDO), under the MRC/FCDO
364 Concordat agreement and is also part of the EDCTP2 programme supported by the
365 European Union. I.D. acknowledges research funding from a Sir Henry Dale Fellowship
366 funded by the Royal Society and Wellcome Trust [grant 213494/Z/18/Z]. V.C. acknowledges
367 funding from the Wellcome Trust [grant 222375/Z/21/Z]. The funders had no role in study
368 design, data collection and analysis, decision to publish, or preparation of the manuscript.

369

370 **Acknowledgements**

371 We would like to acknowledge Sanofi Pasteur for provision of the data used in this research.

372 We acknowledge the participants, their families and the principal investigators involved in the
373 studies.

374 **References**

- 375 1. Brady OJ, Hay SI. The Global Expansion of Dengue: How *Aedes aegypti* Mosquitoes
376 Enabled the First Pandemic Arbovirus . *Annu Rev Entomol.* 2020;65(1):1–18.
- 377 2. Simmons CP, Farrar JJ, van Vinh Chau N, Wills B. Dengue. *N Engl J Med* [Internet].
378 2012 Apr 12;366(15):1423–32. Available from:
379 <http://journals.sagepub.com/doi/10.1177/1461444810365020>
- 380 3. Cattarino L, Rodriguez-Barraquer I, Imai N, Cummings DAT, Ferguson NM. Mapping
381 global variation in dengue transmission intensity. *Sci Transl Med.* 2020;12(528):1–11.
- 382 4. Gibbons R V. Dengue conundrums. *Int J Antimicrob Agents* [Internet].
383 2010;36(SUPPL. 1):S36–9. Available from:
384 <http://dx.doi.org/10.1016/j.ijantimicag.2010.06.019>
- 385 5. Fritzell C, Rousset D, Adde A, Kazanji M, Van Kerkhove MD, Flamand C. Current
386 challenges and implications for dengue, chikungunya and Zika seroprevalence
387 studies worldwide: A scoping review. *PLoS Negl Trop Dis.* 2018;12(7):1–29.
- 388 6. Gubler DJ. Dengue, Urbanization and globalization: The unholy trinity of the 21 st
389 century. *Trop Med Health.* 2011;39(4 SUPPL.):3–11.
- 390 7. Vannice KS, Durbin A, Hombach J. Status of vaccine research and development of
391 vaccines for dengue. *Vaccine* [Internet]. 2016;34(26):2934–8. Available from:
392 <http://dx.doi.org/10.1016/j.vaccine.2015.12.073>
- 393 8. Luo R, Fongwen N, Kelly-Cirino C, Harris E, Wilder-Smith A, Peeling RW. Rapid
394 diagnostic tests for determining dengue serostatus: a systematic review and key
395 informant interviews. *Clin Microbiol Infect* [Internet]. 2019;25(6):659–66. Available
396 from: <https://doi.org/10.1016/j.cmi.2019.01.002>
- 397 9. Kucharski AJ, Kama M, Watson CH, Aubry M, Funk S, Henderson AD, et al. Using

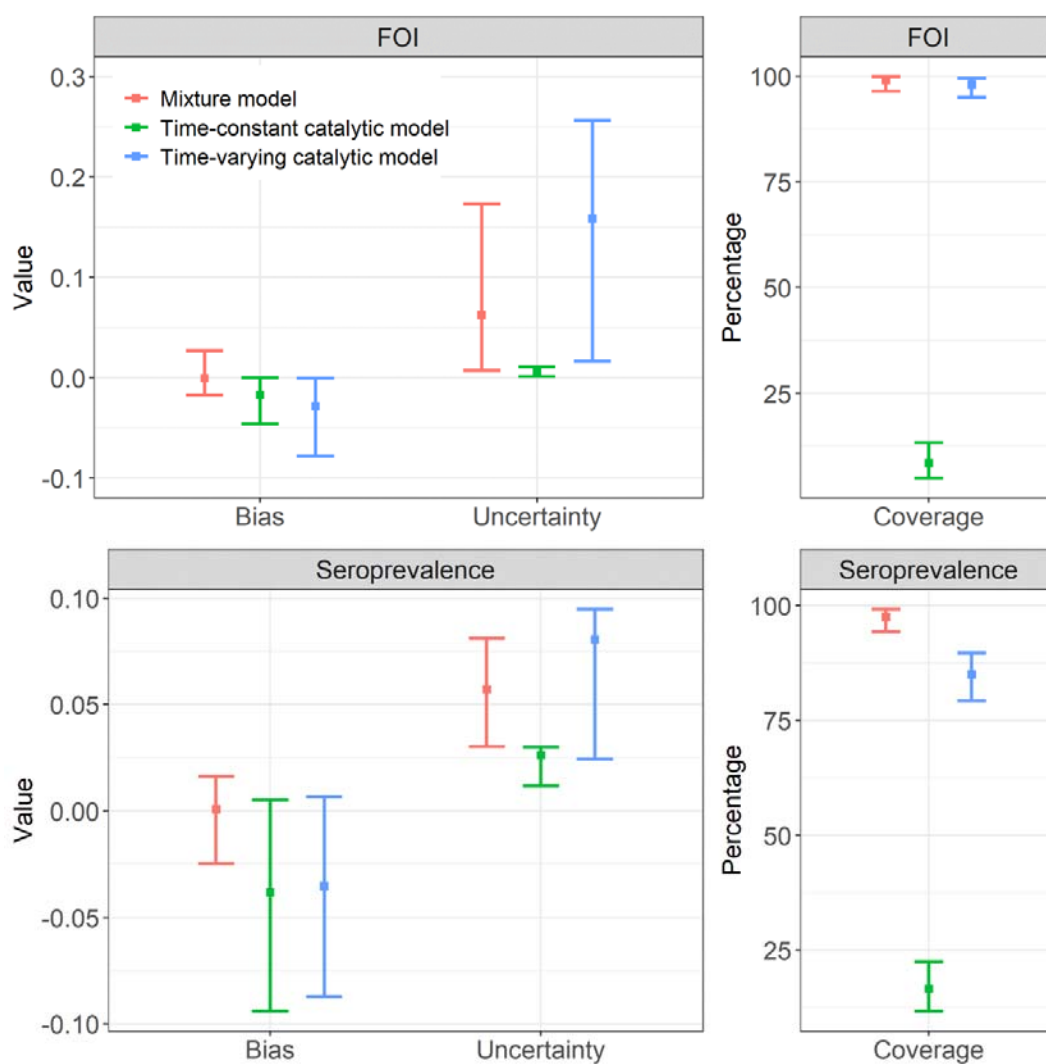
- 398 paired serology and surveillance data to quantify dengue transmission and control
399 during a large outbreak in Fiji. *Elife*. 2018;7:1–26.
- 400 10. O'Reilly KM, Hendrickx E, Kharisma DD, Wilastonegoro NN, Carrington LB, Elyazar
401 IRF, et al. Estimating the burden of dengue and the impact of release of wMel
402 Wolbachia-infected mosquitoes in Indonesia: A modelling study. *BMC Med*.
403 2019;17(1):1–14.
- 404 11. Lauer SA, Sakrejda K, Ray EL, Keegan LT, Bi Q, Suangtho P, et al. Prospective
405 forecasts of annual dengue hemorrhagic fever incidence in Thailand, 2010–2014.
406 *Proc Natl Acad Sci U S A*. 2018;115(10):E2175–82.
- 407 12. O'Driscoll M, Imai N, Ferguson N, Hadinegoro SR, Satari HI, Tam C, et al.
408 Spatiotemporal Variability in Dengue Transmission Intensity in Jakarta, Indonesia.
409 2018;1–62.
- 410 13. Hens N, Aerts M, Faes C, Shkedy Z, Lejeune O, Van Damme P, et al. Seventy-five
411 years of estimating the force of infection from current status data. *Epidemiol Infect*.
412 2010;138(6):802–12.
- 413 14. Ferguson NM, Donnelly CA, Anderson RM. Transmission dynamics and epidemiology
414 of dengue: Insights from age-stratified sero-prevalence surveys. *Philos Trans R Soc B
415 Biol Sci*. 1999;354(1384):757–68.
- 416 15. Grenfell BYBT, Anderson RM. The estimation of age-related rates of infection from
417 case notifications and serological data. 1985;(1985):419–30.
- 418 16. Nokes BYDJ, Anderson RM. Rubella epidemiology in South East England.
419 1986;(1986):291–304.
- 420 17. Schenze D, Dietz K, Frösner G. Antibody against Hepatitis A in Seven European
421 Countries: II. Statistical Analysis of Cross-Sectional surveys. *Am J Epidemiol*
422 [Internet]. 1979;10(1):70–76. Available from:

- 423 <https://academic.oup.com/aje/article/110/1/70/62356>
- 424 18. Delgado S, Neyra RC, Machaca VRQ, Juárez JA, Chu LC, Verastegui MR, et al. A
425 history of Chagas disease transmission, control, and re-emergence in peri-rural La
426 Joya, Peru. *PLoS Negl Trop Dis*. 2011;5(2).
- 427 19. Imai N, Dorigatti I, Cauchemez S, Ferguson NM. Estimating Dengue Transmission
428 Intensity from Sero-Prevalence Surveys in Multiple Countries. *PLoS Negl Trop Dis*
429 [Internet]. 2015;9(4):1–19. Available from:
430 <http://dx.doi.org/10.1371/journal.pntd.0003719>
- 431 20. Salje H, Paul KK, Paul R, Rodriguez-Barraquer I, Rahman Z, Alam MS, et al.
432 Nationally-representative serostudy of dengue in Bangladesh allows generalizable
433 disease burden estimates. *Elife*. 2019;8:1–17.
- 434 21. Rodriguez-Barraquer I, Salje H, Cummings DA. Opportunities for improved
435 surveillance and control of dengue from age-specific case data. *Elife*. 2019;8.
- 436 22. Bollaerts K, Aerts M, Shkedy Z, Faes C, Beutels P, Hens N. of infection directly from
437 antibody titres ER ER. *Stat Modelling*. 2012;12(5):441–62.
- 438 23. Vink MA, Kasstele J Van De, Wallinga J, Teunis PFM, Bogaards JA. Estimating
439 Seroprevalence of Human Papillomavirus Type 16 Using a Mixture Model with
440 Smoothed Age-dependent Mixing Proportions. 2015;26(1).
- 441 24. Hens N, Shkedy Z, Aerts M, Faes C, Damme P Van, Beutels P. Modeling Infectious
442 Disease Parameters Based on Serological and Social Contact Data: A Modern
443 Statistical Perspective (Google eBook). 2012;314. Available from:
444 <http://books.google.com/books?id=IH08pTAoe6QC&pgis=1>
- 445 25. Gay NJ. Analysis of serological surveys using mixture models: Application to a survey
446 of parvovirus B19. *Stat Med*. 1996;15(14):1567–73.
- 447 26. Hardelid P, Williams D, Dezateux C, Tookey PA, Peckham CS, Cubitt WD, et al.

- 448 Analysis of rubella antibody distribution from newborn dried blood spots using finite
449 mixture models. *Epidemiol Infect.* 2008;136(12):1698–706.
- 450 27. Rota MC, Massari M, Gabutti G, Guido M, De Donno A, Atti MLC degli. Measles
451 serological survey in the Italian population: Interpretation of results using mixture
452 model. *Vaccine.* 2008;26(34):4403–9.
- 453 28. Chisenga CC, Bosomprah S, Musukuma K, Mubanga C, Chilyabanyama ON, Velu
454 RM, et al. Sero-prevalence of arthropod-borne viral infections among Lukanga swamp
455 residents in Zambia. *PLoS One* [Internet]. 2020;15(7):1–13. Available from:
456 <http://dx.doi.org/10.1371/journal.pone.0235322>
- 457 29. Biggs JR, Sy AK, Brady OJ, Kucharski AJ, Funk S, Reyes MAJ, et al. A serological
458 framework to investigate acute primary and post-primary dengue cases reporting
459 across the Philippines. *BMC Med.* 2020;18(1):1–14.
- 460 30. Tien NTK, Luxemburger C, Toan NT, Pollissard-Gadroy L, Huong VTQ, Van Be P, et
461 al. A prospective cohort study of dengue infection in schoolchildren in Long Xuyen,
462 Viet Nam. *Trans R Soc Trop Med Hyg* [Internet]. 2010;104(9):592–600. Available
463 from: <http://dx.doi.org/10.1016/j.trstmh.2010.06.003>
- 464 31. Prayitno A, Taurel AF, Nealon J, Satari HI, Karyanti MR, Sekartini R, et al. Dengue
465 seroprevalence and force of primary infection in a representative population of urban
466 dwelling Indonesian children. *PLoS Negl Trop Dis.* 2017;11(6):1–16.
- 467 32. R Core Team. R: A language and environment for statistical computing. [Internet].
468 2019. Available from: <https://www.r-project.org/>
- 469 33. Rodriguez-Barraquer I, Cordeiro MT, Braga C, de Souza W V., Marques ET,
470 Cummings DAT. From re-emergence to hyperendemicity: The natural history of the
471 dengue epidemic in Brazil. *PLoS Negl Trop Dis.* 2011;5(1):1–7.
- 472 34. Macdonald P, Du J. mixdist: Finite Mixture Distribution [Internet]. 2018. Available

- 473 from: <https://cran.r-project.org/package=mixdist>, package version 0.5-5.0A
- 474 35. Eilers PHC, Marx BD, Ellers PHC. Linked references are available on JSTOR for this
475 article: Flexible Smoothing with B-splines and Penalties. *Stat Sci.* 1996;11(2):89–
476 102.
- 477 36. Kovac T. *serostat: Modeling Infectious Disease Parameters Based on Serological and*
478 *Social Contact.* 2018.
- 479 37. Rabaa MA, Simmons CP, Fox A, Le MQ, Nguyen TTT, Le HY, et al. Dengue Virus in
480 Sub-tropical Northern and Central Viet Nam: Population Immunity and Climate Shape
481 Patterns of Viral Invasion and Maintenance. *PLoS Negl Trop Dis.* 2013;7(12).
- 482 38. Kafatos G, Andrews NJ, Conway KJMC, Maple PAC. Is it appropriate to use fixed
483 assay cut-offs for estimating seroprevalence? 2016;(2016):887–95.
- 484 39. Tam CC, O'Driscoll M, Taurel AF, Nealon J, Hadinegoro SR. Geographic variation in
485 dengue seroprevalence and force of infection in the urban paediatric population of
486 Indonesia. *PLoS Negl Trop Dis.* 2018;12(11):1–12.
- 487 40. Thai KTD, Binh TQ, Giao PT, Phuong HL, Hung LQ, Van Nam N, et al.
488 Seroprevalence of dengue antibodies, annual incidence and risk factors among
489 children in southern Vietnam. *Trop Med Int Heal.* 2005;10(4):379–86.
- 490
- 491

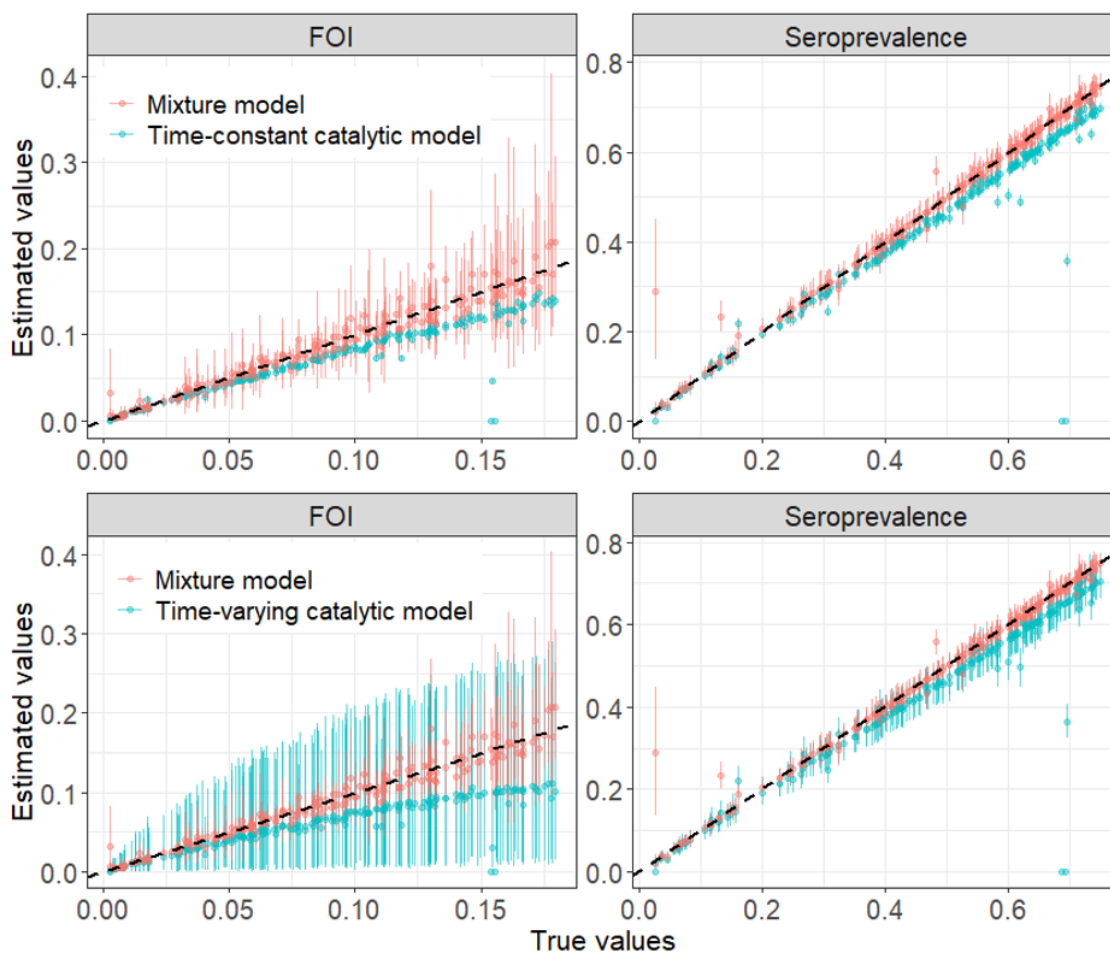
492 **Figure 1: Bias, coverage, and degree of uncertainty for seroprevalence and force of**
493 **infection (FOI) estimates using catalytic and mixture models fitted to simulated**
494 **datasets (Dataset C).** Bias is calculated as the estimated parameter value minus the true
495 parameter value. Uncertainty is the width of the 95% Confidence intervals (CIs) around the
496 central estimates, calculated using the bootstrap method. The coverage is the percentage of
497 simulations where the estimated CIs contained the true values. For the bias and the
498 uncertainty, the mean and 95% CI across the 200 simulations are given. For the coverage,
499 the 95% exact binomial CI are given. Note that the y-axis limits differ for each panel.



500

501

502 **Figure 2: True versus estimated seroprevalence and force of infection (FOI) values**
503 **from the mixture and catalytic models fitted to the simulated datasets (Dataset C).** The
504 catalytic model was run under the assumption that the FOI was time-constant or time-
505 varying. The 95% Confidence Intervals for the estimated values were calculated using a
506 bootstrap method and are shown here as error bars; the point denotes the central estimate.



507

508

509

510

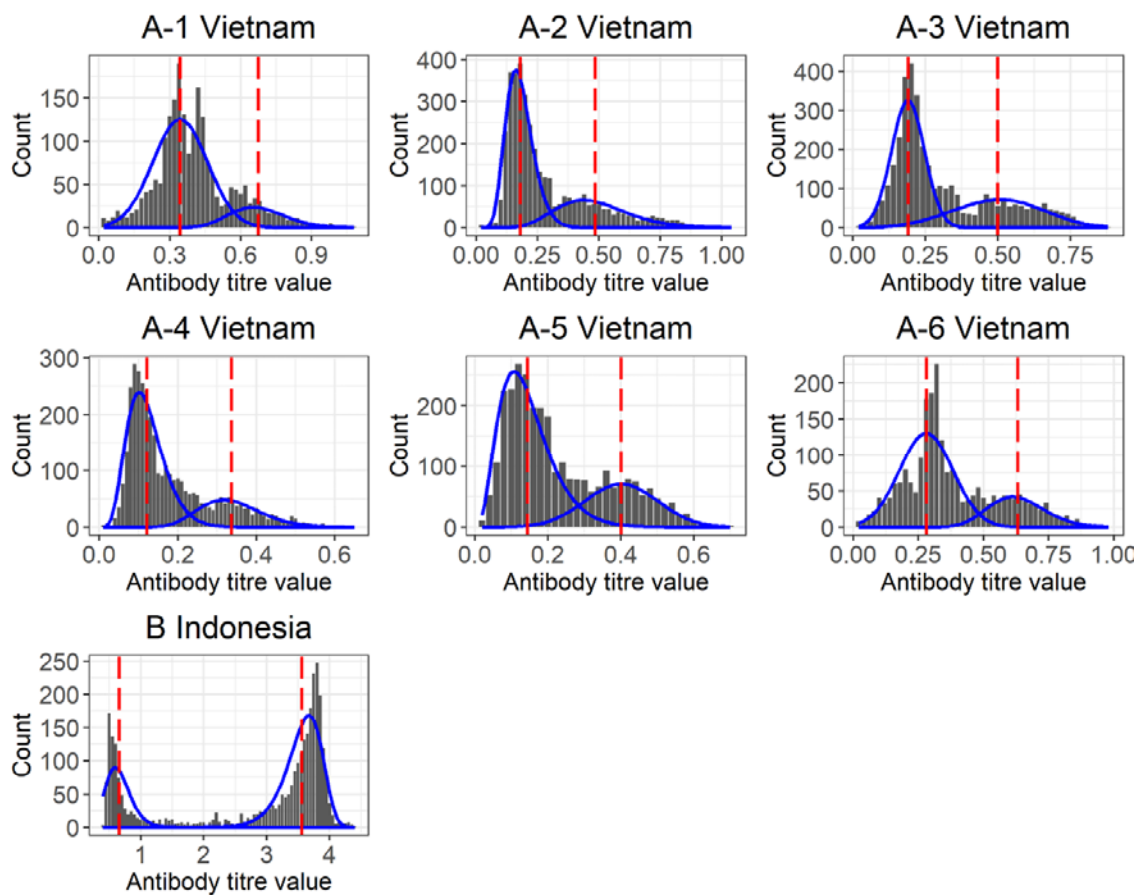
511

512

513

514 **Figure 3: Mixture model fitted to the Vietnamese (A1:A6) and Indonesian (B) datasets.**

515 The distribution of $\log(\text{titre}+1)$ is shown in dark grey, the fitted mixture model is shown in
516 blue, and the red dashed lines represent the mean antibody titre of each component of the
517 fitted mixture model (μ_s and μ_t for the seronegative and seropositive components
518 respectively). Note that the y-axis limits differ for each panel.



519

520

521

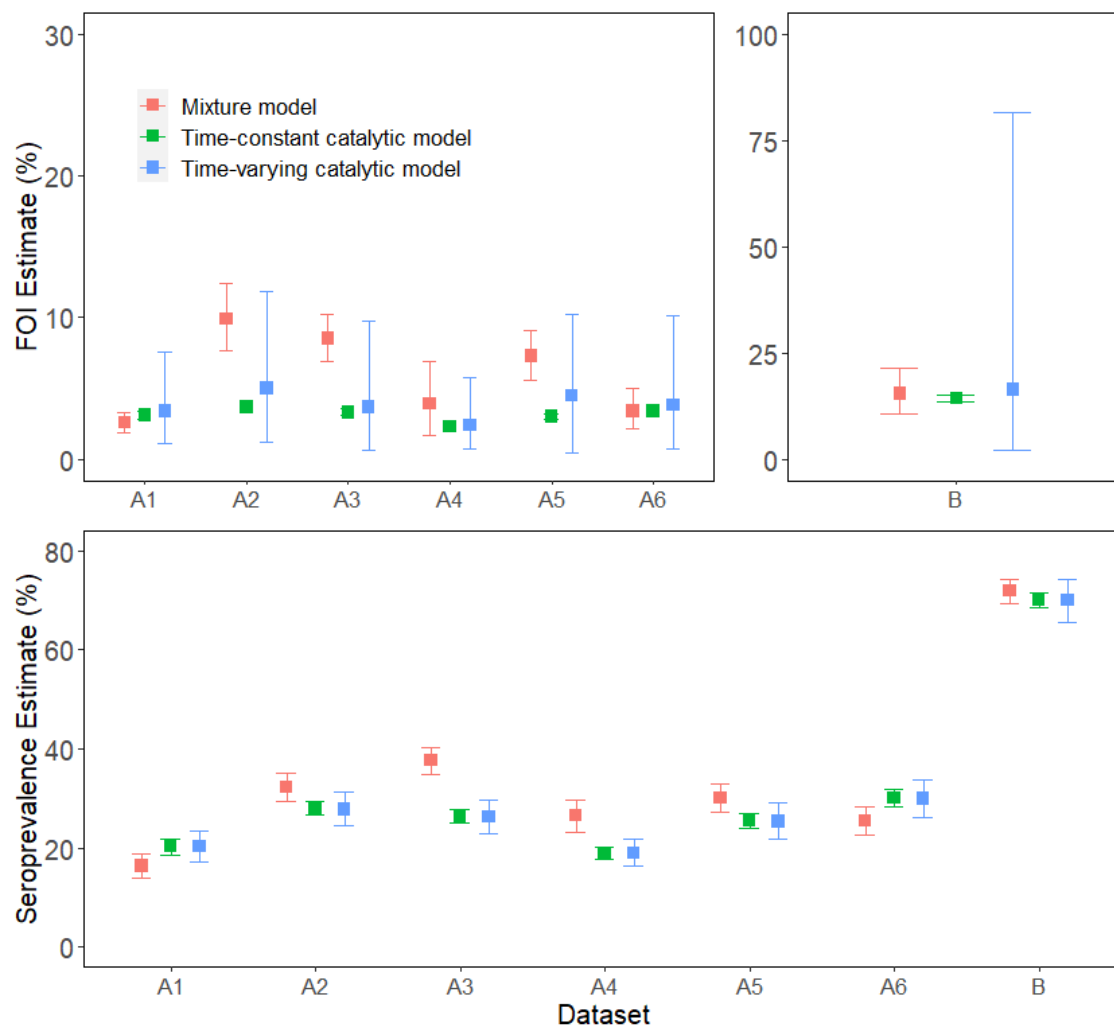
522

523

524

525

526 **Figure 4: Force of infection (FOI) and total population level seroprevalence (SP)**
527 **estimates from the mixture model and the catalytic models fitted to the observed data.**
528 The catalytic model was run under the time-constant and time-varying FOI assumption. The
529 95% Confidence Intervals (CI) which were calculated by bootstrapping for all models are
530 given as error bars. Note that the y-axis limits differ for each panel.



531

532

533

534

535

536

537 **Figure 5: Age-specific seroprevalence estimates for the IgG data from Vietnam**
538 **(Dataset A1:A6) and from Indonesia (Dataset B) aggregated across all subdistricts.**
539 Mixture model estimates are in blue, catalytic model estimates are in orange and green
540 when applied under the assumption that the FOI is time-constant or time-varying
541 respectively. Shading represents the 95% Confidence Intervals (CI). The grey points show
542 the observed seroprevalence per age group calculated from the binarily classified IgG data
543 (seropositive individuals / tested individuals), with error bars indicating the 95% exact
544 binomial CIs. The seroprevalence data and model estimates are overlaid for the purpose
545 of comparison. However, it is important to note that the mixture model was not fitted to the
546 data (grey points), as the former does not depend on the titre classification. The size of the
547 grey data points represents the number of individuals tested in each age group.

